



ELSEVIER

Journal of Alloys and Compounds 323–324 (2001) 444–447

Journal of
ALLOYS
AND COMPOUNDS

www.elsevier.com/locate/jallcom

Synthesis, characterization, magnetism and transport properties of $\text{Nd}_{1-x}\text{Sr}_x\text{CoO}_3$ perovskites

A. Fondado^{a,*}, M.P. Breijo^b, C. Rey-Cabezudo^b, M. Sánchez-Andújar^b, J. Mira^a, J. Rivas^a,
M.A. Señarís-Rodríguez^b

^aDepartment Física Aplicada, Universidad de Santiago de Compostela, 15706 Santiago de Compostela, Spain

^bDepartment Química Fundamental, Universidad de A Coruña, 15071 A Coruña, Spain

Abstract

We have prepared polycrystalline, single-phase $\text{Nd}_{1-x}\text{Sr}_x\text{CoO}_3$ materials ($0 \leq x \leq 0.40$) using the nitrate decomposition method and we have studied how their structural, magnetic and transport properties change upon Sr^{2+} doping. In this context we find that these series of compounds crystallize in GdFeO_3 -type perovskite structures whose cell volume increases as x gets higher. From the magnetic point of view, this doping makes the materials evolve towards a ferromagnetic behavior as x increases, so that for $x > 0.20$ the samples are already ferromagnetic below a $T_c \sim 225$ K. Also, their electrical conductivity progressively increases with x . Nevertheless the materials remain semiconducting for $x \leq 0.30$ and only the sample with $x = 0.40$ displays a M–I transition as a function of temperature ($T_{MI} \sim 160$ K). © 2001 Elsevier Science B.V. All rights reserved.

Keywords: Crystal structure and symmetry; Magnetic measurements; Electronic transport

1. Introduction

The $\text{Ln}_{1-x}\text{Sr}_x\text{CoO}_3$ perovskite oxides are systems that are known to exhibit compositionally controlled paramagnetic–ferromagnetic transitions as well as metal–insulator transitions [1–6]. In addition, spin transitions at the cobalt ions — that take place as a function of temperature and doping — make these systems more complex [2,7].

Of all $\text{Ln}_{1-x}\text{Sr}_x\text{CoO}_3$ series of compounds, the lanthanum $\text{La}_{1-x}\text{Sr}_x\text{CoO}_3$ perovskites have been most thoroughly investigated. In this system, while the parent compound LaCoO_3 shows high resistivity and antiferromagnetic exchange interactions [8], upon doping the materials tend to metallic and ferromagnetic behavior [1]. The evolution takes place smoothly, and a number of different magnetic and electrical behaviors have been described for the intermediate degrees of doping [2,9]. More recently, magnetoresistive effects have also been observed in this system [10,11].

Other $\text{Ln}_{1-x}\text{Sr}_x\text{CoO}_3$ (Ln: rare earth) systems are also known to show similarly interesting magnetic and electrical properties, that are influenced by the nature of the rare-earth ion [3,4]. Although the general trend is, again, that the materials tend to ferromagnetic and metallic

behavior as x increases, the characteristics of such evolution have been relatively much less studied.

It is in one of these systems, $\text{Nd}_{1-x}\text{Sr}_x\text{CoO}_3$, in which we focus our studies.

2. Experimental

$\text{Nd}_{1-x}\text{Sr}_x\text{CoO}_3$ materials ($0 \leq x \leq 0.50$) were prepared by decomposition of the corresponding mixture of nitrates using Nd_2O_3 , SrCO_3 , $\text{Co}(\text{NO}_3)_2 \cdot 6\text{H}_2\text{O}$ and nitric acid (30%) as starting materials. The obtained precursor powders were pressed into pellets and heated in air at 950°C for 24 h and finally cooled slowly to room temperature ($0.7^\circ\text{C}/\text{min}$).

The samples were characterized by X-ray powder diffraction with a Siemens D-5000 diffractometer and $\text{Cu}(\text{K}_\alpha) = 1.5418 \text{ \AA}$ radiation, and by scanning electron microscopy (SEM) using a Jeol 6400 microscope.

Their thermal stability was checked by differential thermal analysis (DTA) and thermogravimetric analyses (TGA).

Magnetic properties were studied in a DMS-1660 vibrating-sample magnetometer. Zero-field-cooled (ZFC) and field-cooled (FC) magnetic susceptibility data were obtained in a field of 1000 Oe from 77 to 330 K. ZFC

*Corresponding author.

magnetization curves $M(H)$ were obtained with fields ± 13 kOe at 77 K.

Four-probe electrical resistivity and Seebeck coefficients of pressed pellets were measured in the temperature ranges $77 \text{ K} \leq T \leq 300 \text{ K}$ and $77 \text{ K} \leq T \leq 450 \text{ K}$, respectively.

3. Results and discussion

3.1. Sample characterization

According to their room-temperature X-ray diffraction patterns, the obtained $\text{Nd}_{1-x}\text{Sr}_x\text{CoO}_3$ samples are single-phase materials for Sr^{2+} doping $0 \leq x \leq 0.40$. Nevertheless for $x=0.50$ the main phase appears impurified by small amounts of $\text{SrCoO}_{3-\delta}$. (So, hereafter we will focus only in the compositions $0 \leq x \leq 0.40$).

These polycrystalline materials consist of small homogeneous particles with averaged diameter $0.5 \mu\text{m}$, as shown by SEM micrographs. These relatively small particle size values are the result of moderate temperatures and relatively short heating treatments used for the synthesis of these materials.

According to the thermogravimetric results, these samples lose some oxygen on heating above 600 K. For lower Sr^{2+} content, $x \leq 0.20$, oxygen is completely recuperated upon slow cooling in air, but for $x > 0.20$, the oxygen loss is more pronounced and only 98.5–99% of the initial oxygen content is recuperated under these conditions, so those samples are slightly oxygen deficient.

As for their crystal structure, the X-ray diffraction patterns can be indexed on the basis of a GdFeO_3 -type perovskite (S.G. Pbnm) [12]. The samples with $x \leq 0.20$ are pseudo-tetragonal ($a \cong b$), while the samples with $x > 0.20$ are O-type orthorhombic ($a \leq c/\sqrt{2} \leq b$).

It is interesting to note that the cell volume is seeing to increase with x (Fig. 1), the effect being more pronounced for $0 < x \leq 0.20$. This expansion of the unit cell indicates that the incorporation of the larger size Sr^{2+} ion ($r_{\text{Sr}^{2+}}^{\text{XII}} = 1.44 \text{ \AA}$) in place of the considerably smaller Nd^{3+} ion ($r_{\text{Nd}^{3+}}^{\text{XII}} = 1.27 \text{ \AA}$) (13) predominates over the fact that upon doping Co^{3+} ($r_{\text{Co}^{3+}}^{\text{VI}} = 0.55 \text{ \AA}$, $r_{\text{Co}^{3+}}^{\text{VI}} = 0.61 \text{ \AA}$) [13] oxidates to the smaller Co^{4+} ions ($r_{\text{Co}^{4+}}^{\text{VI}} = 0.53 \text{ \AA}$) [13].

3.2. Magnetic properties

NdCoO_3 is paramagnetic and its $\chi(T)$ data follow the Curie–Weiss law for $T < 250 \text{ K}$. From the corresponding $\chi^{-1}(T)$ fitting, the effective magnetic moment per cobalt ion ($\mu_{\text{eff-Co}}$) was calculated from the total $\mu_{\text{eff}} = \sqrt{8C}$ after appropriate subtraction of the Nd^{3+} contribution ($\mu_{\text{eff}}(\text{Nd}^{3+}) = 3.8 \mu_{\text{B}}$). The obtained value, $\mu_{\text{eff-Co}} = 0$, indicates that the trivalent cobalt ions are in the low spin configuration ($t_{2g}^6 e_g^0$) in this temperature interval. If we

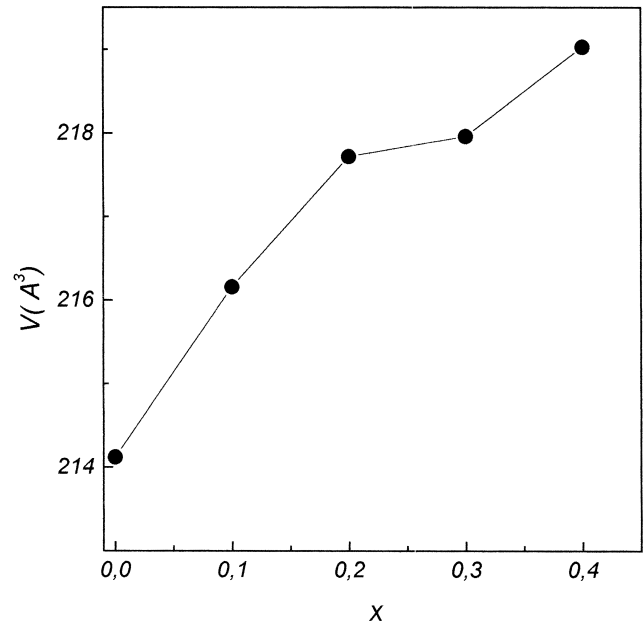


Fig. 1. Variation of the unit cell volume of $\text{Nd}_{1-x}\text{Sr}_x\text{CoO}_3$ compounds as a function of x .

compare this result with that corresponding to LaCoO_3 [2], we see that in the Nd-compound the Co(III) ions remain low spin over a larger temperature interval. This fact is related to the bigger acidity of the Nd^{3+} ion with respect to La^{3+} , which causes an increase in the crystal field splitting Δ_{cr} [14] in the NdCoO_3 compound.

At $T > 250 \text{ K}$ a deviation from linearity appears in the $\chi^{-1}(T)$ plot, that would indicate the onset of a spin transition at the cobalt ions, as it has been shown by other authors that made magnetic studies over larger temperature intervals [15,16].

Upon Sr^{2+} substitution the magnetic susceptibility of these compounds increases markedly and the materials evolve towards ferromagnetic behavior (Fig. 2(a)). In this context, ferromagnetism is found in samples with $x > 0.20$ below a Curie temperature $T_c \approx 225 \text{ K}$, that changes very little with x . These results are at difference with those previously described in the literature for ceramic samples prepared at higher temperatures ($1127\text{--}1227^\circ\text{C}$) (3), in which the reported T_c are smaller than these and clearly increase with x . For example, the Curie temperature reported for the ceramic sample with $x=0.40$ is only $90 \pm 10 \text{ K}$ and increases to $190 \pm 15 \text{ K}$ for $x=0.50$, a higher value that nevertheless is still smaller than the $T_c = 240 \text{ K}$ displayed by our samples. In this context, variations in the oxygen content of the compared samples could be responsible for the observed differences.

From these $\chi(T)$ curves we can obtain information about the spin state of the Co ions only in the case of the non-ferromagnetic lower doped samples ($x \leq 0.10$). In those compounds the Curie–Weiss law is again obeyed for $77 < T < 250 \text{ K}$, a deviation from linearity appearing for

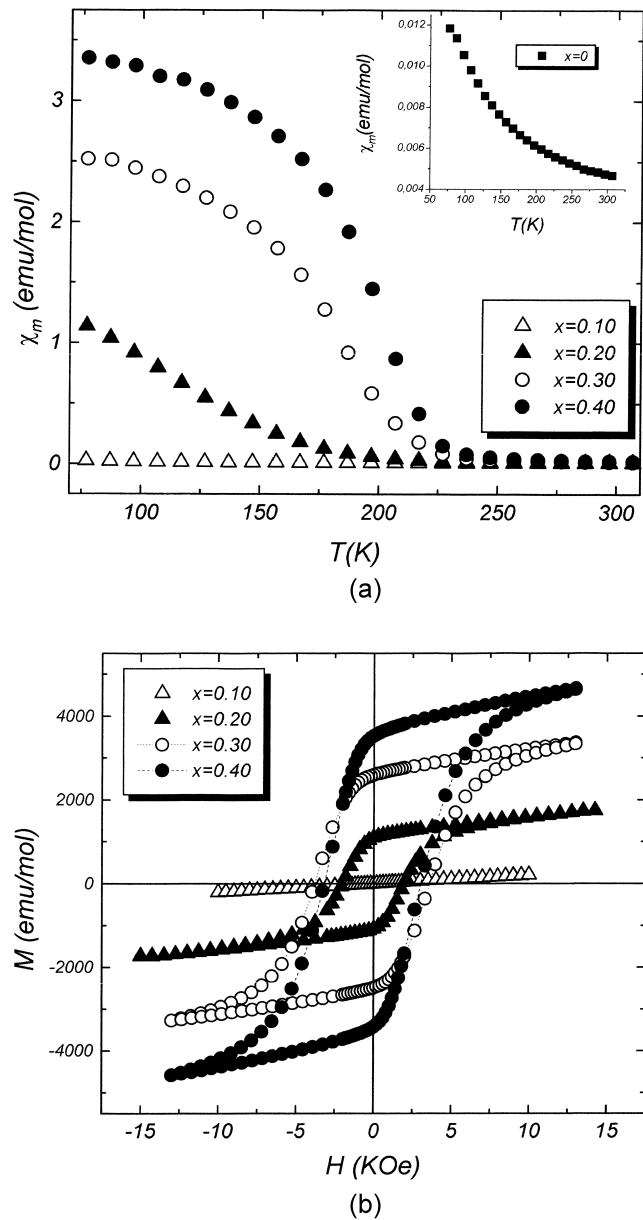


Fig. 2. (a) FC molar magnetic susceptibility of $\text{Nd}_{1-x}\text{Sr}_x\text{CoO}_3$ samples, $0 \leq x \leq 0.40$ (the data for $x=0$ are shown in the inset) and (b) ZFC magnetization versus applied field H , measured at 77 K, of $\text{Nd}_{1-x}\text{Sr}_x\text{CoO}_3$ samples, $0 < x \leq 0.40$.

$T > 250$ K. The obtained effective magnetic moments per cobalt ion ($\mu_{\text{eff-Co}}$) indicate that in the lower temperature interval the cobalt ions are in the low spin configuration, an evolution towards a higher spin configuration taking place at $T > 250$ K, as in the undoped compound.

As for the $M(H)$ curves corresponding to the ferromagnetic samples (Fig. 2(b)), they show, first of all, that the values of maximum magnetization increase with x and that at 77 K none of them reaches saturation under the maximum field used of $H = 13$ kOe. They also indicate that the $x > 0.20$ samples are hard ferromagnetic materials: their coercive fields are very high, the maximum value is

achieved for $x = 0.30$ ($H_c = 3800$ Oe), and then decreases to 3200 and 2400 Oe for $x = 0.40$ and 0.20, respectively; they also show high remnant magnetization values ($M_{\text{rem}} = 3520$ emu/mol for $x = 0.40$). Both magnitudes are much higher than in the corresponding $\text{La}_{1-x}\text{Sr}_x\text{CoO}_3$ compounds [2].

Taking into account that, at difference with La^{3+} that has $L = S = 0$, Nd^{3+} has a high value of L ($L = 6$) and an $S = 3/2$, we interpret these results as an evidence of the contribution of the L - S coupling in the rare earth ion to the magnetic anisotropy of the system.

3.3. Transport properties

Both the resistivity and Seebeck coefficient measurements show that the electrical conductivity of NdCoO_3 drastically increases upon Sr^{2+} doping, so that the higher x the lower is their resistivity (Figs. 3 and 4). The Seebeck results also reveal that the charge carriers are holes (the sign of the Seebeck coefficient is positive) and that their number increases with x (the Seebeck coefficients get smaller) (Fig. 4).

Nevertheless, for these doping degrees ($0 < x \leq 0.40$) the metallic regime is not achieved: the samples with $x \leq 0.30$ are semiconducting and the sample with $x = 0.40$, whose conductivity is very close to the minimum metallic conductivity σ_{min} ($10^3 \Omega^{-1} \text{cm}^{-1}$) [17], displays a M-I transition as a function of temperature, $T_{\text{MI}} \sim 160$ K (Fig. 3).

For the samples $x \leq 0.30$, in which the electrical conductivity is thermally activated in the temperature range

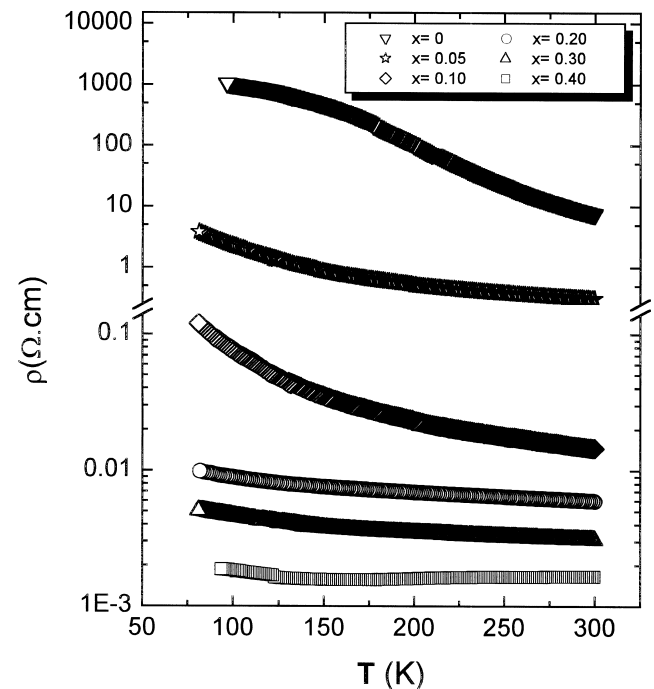


Fig. 3. Resistivity versus temperature curves of $\text{Nd}_{1-x}\text{Sr}_x\text{CoO}_3$ samples, $0 \leq x \leq 0.40$.

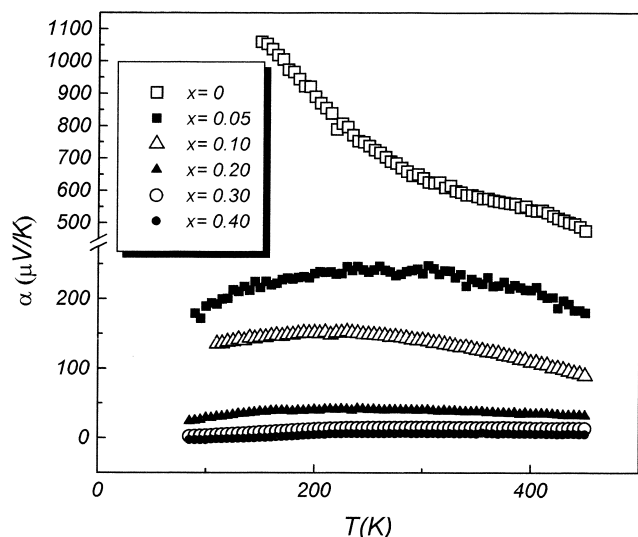


Fig. 4. Thermoelectric power, α , of $\text{Nd}_{1-x}\text{Sr}_x\text{CoO}_3$ samples, $0 \leq x \leq 0.40$, as a function of temperature.

studied, we have calculated activation energies from the linear parts of the $\ln \sigma$ vs. $1/T$ plots (Fig. 5). The measured E_{act} , that is much larger in the undoped compound, 0.3 eV, clearly diminishes upon doping: it decreases from 0.04 eV for $x=0.05$ to 0.01 eV for $x=0.30$.

These results can be understood on the basis of the electronic structure of this type of compounds. In the undoped compound, where the Co(III) ions are all low spin for $T < 250$ K, the electronic structure would be essentially similar to the one described for LaCoO_3 for $T < 77$ K [8]: it would consist of π^* band states at the top of the O-2p valence band (that result from strong hybridization of the cobalt orbitals of t_{2g} parentage with the O-2p orbitals), that are completely full; separated from these and at higher energies there is a σ^* band (that results from

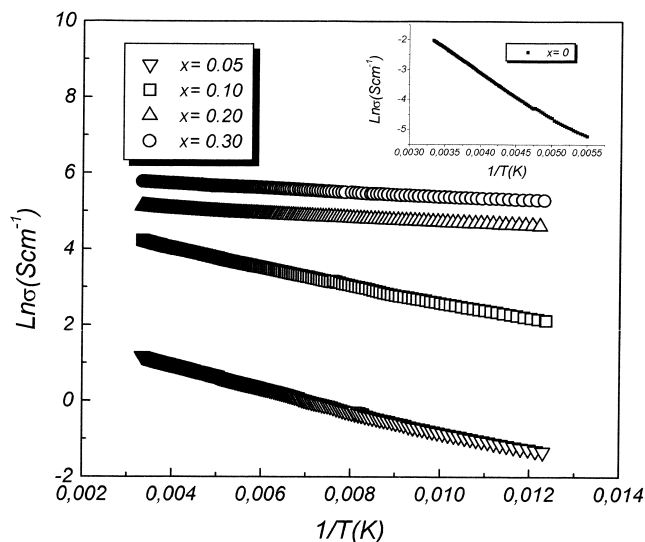


Fig. 5. Plots of $\ln \sigma$ vs. $1/T$ for the system $\text{Nd}_{1-x}\text{Sr}_x\text{CoO}_3$, $0 \leq x < 0.40$ (the data for $x=0$ are shown in the inset).

σ -bonding orbitals of e parentage) that is completely empty. And due to the bigger acidity of the Nd^{3+} ion compared to La^{3+} , the separation between the π^* band and the σ^* band will be bigger and the bands will be narrower than in LaCoO_3 [8].

Thus, the activation energy calculated in this region, that represents the energy required to promote a t_{2g} electron to the σ^* band, is bigger than in LaCoO_3 [18] and the sample resistivity is higher.

As for the doped materials, the substitution of Sr^{2+} for Nd^{3+} oxidizes the CoO_3 array and creates, formally, low spin Co(IV): $t_{2g}^5 e_g^0$ configurations within a strongly covalent CoO_3 site complex. Thus, the much lower E_{act} found in these doped compounds, would represent the energy for the movement of the already existing holes through the π^* band. It is also worth noting that as this π^* band is narrower than in the corresponding La-compounds, the semiconducting regime extends over a larger compositional interval in this $\text{Nd}_{1-x}\text{Sr}_x\text{CoO}_3$ system.

Acknowledgements

We thank Spanish DGICYT for financial support under project MAT98-0416-C03-02.

References

- [1] P.M. Raccach, J.B. Goodenough, J. Appl. Phys. 39 (1968) 1209.
- [2] M.A. Señarís-Rodríguez, J.B. Goodenough, J. Solid State Chem. 118 (1995) 323.
- [3] C.N.R. Rao, O.M. Parkash, D. Bahadur, P. Ganguly, A. Nagabhu Share, J. Solid State Chem. 22 (1977) 353.
- [4] C.N.R. Rao, O.M. Parkash, Philosophical Magazine 35 (1977) 1111.
- [5] G.Ch. Kostoglouidis, N. Vasilakos, Ch. Fitkos, Solid State Ionics 106 (1998) 207.
- [6] K.H. Ryu, K.S. Roh, S.J. Lee, C.H. Yo, J. Solid State Chem. 105 (1993) 550.
- [7] P.M. Raccach, J.B. Goodenough, Phys. Rev. 155 (1967) 932.
- [8] M.A. Señarís-Rodríguez, J.B. Goodenough, J. Solid State Chem. 116 (1995) 224.
- [9] M. Itoh, I. Natori, S. Kubota, K. Matoya, J. Phys. Soc. Jpn. 63 (1994) 1486.
- [10] V. Golovanov, L. Mihaly, A.R. Moodenbaugh, Phys. Rev. B 53 (1996) 8207.
- [11] R. Mahendiram, K. Raychaudhuri, Phys. Rev. B 54 (1996) 16044.
- [12] S. Geller, J. Chem. Phys. 24 (1956) 1236.
- [13] R.D. Shannon, C.T. Prewitt, Acta Crystallogr. Sect. B 25 (1969) 925.
- [14] G. Demazeau, M. Pouchard, P. Hagenmuller, J. Solid State Chem. 9 (1974) 202.
- [15] D.S. Rajoria, V.G. Bhide, G. Rama Rao, C.N.R. Rao, J. Chem. Soc. Faraday Trans. II 70 (1974) 512.
- [16] W.H. Madhusudan, K. Jagannathan, P. Ganguly, C.N.R. Rao, J. Chem. Soc. Dalton Trans. 1397 (1980).
- [17] C.N.R. Rao, P. Ganguly, in: P.P. Edward, C.N.R. Rao (Eds.), The Metallic and Non-metallic States of Matter, Taylor & Francis, London, 1985.
- [18] E. Iguchi, K. Ueda, W.H. Jung, Phys. Rev. B 54 (1996) 17431.